

ARTICLES

Side-Chain Polymer Liquid Crystals Containing Oxadiazole and Amine Moieties with Carrier-Transporting Abilities for Single-Layer Light-Emitting Diodes

Masuki Kawamoto, Hiroyuki Mochizuki, Atsushi Shishido, Osamu Tsutsumi, Tomiki Ikeda,*
Bong Lee,[†] and Yasuhiko Shirota[‡]

*Chemical Resources Laboratory, Tokyo Institute of Technology, 4259 Nagatsuta,
Midori-ku, Yokohama 226-8503, Japan, Department of Polymer Engineering,
Pukyong National University, Korea, and Department of Applied Chemistry,
Faculty of Engineering, Osaka University, Yamadaoka, Suita, Osaka 565-0871, Japan*

Received: July 10, 2002; In Final Form: November 15, 2002

Electrochemical and electroluminescent (EL) properties of a polymer liquid crystal (PLC) composed of an oxadiazole moiety as an electron-transporting unit and an amine moiety as a hole-transporting unit in the same side chain were investigated. It has been found that the polymer is a good candidate for a single-layer light-emitting diode (LED) because it combines carrier-transporting and emission properties in a single species. A polymer LED was fabricated with a simple configuration of ITO/PLC/MgAg to demonstrate EL behavior. The device showed the EL emission in a blue region with a maximum brightness of 13 cd/m² at 26 V. Furthermore, a polarized EL emission was observed due to self-assemblies of mesogenic chromophores. The dichroic ratio of the absorption of the polymer film determined by polarized absorption spectra measured with the polarized beam parallel and perpendicular to the rubbing direction was 1.8, and the dichroic ratio of the emission was estimated to be 1.6. These results clearly indicate that the origin of the polarized emission from the polymer film is the anisotropic arrangement of the mesogenic chromophores.

Introduction

Organic light-emitting diodes (LEDs) have received a great deal of attention for their application as full-color, flat-panel displays.¹ The basic configuration of LEDs is composed of thin films of organic materials sandwiched between two electrodes. Low-molecular-weight materials may form thin films by vapor deposition. This preparation method to build electroluminescent (EL) devices was first developed by Tang and VanSlyke.² In the development of high-performance EL devices, the key

requirement is the preparation of thin films without grain boundaries and with large-scale perfect domains. Amorphous molecular materials are a current topic because of their glass-forming property, which leads to the formation of smooth and uniform thin films.^{1c,3} On the other hand, polymer materials are generally expected to be suitable for LEDs because they have good processability, simple fabrication by solution processes, and an intrinsically high durability.⁴ In general, light-emitting polymers are rarely good conductors for both electrons and holes, whereas LED devices require balanced injection and transport of both of them. Unfortunately, most of the polymers developed so far transport electrons much less efficiently than holes, which significantly decreases the efficiency of the devices. To facilitate the charge-injection and -transporting abilities,

* To whom correspondence should be addressed. Phone: +81-45-924-5240. FAX: +81-45-924-5275. E-mail: tiked@res.titech.ac.jp. WWW: <http://www.res.titech.ac.jp/polymer>.

[†] Pukyong National University.

[‡] Osaka University.

multilayer devices have been developed. Such an approach has been very successful in improving device efficiency and stability.⁵

Single-layer LEDs can be fabricated much more easily than multilayer LEDs, even though multilayer devices have been found to be more efficient than single-layer ones. To overcome this problem, blended materials that contain mixtures of hole transporters, electron transporters, and emitters have often been used to prepare efficient single-layer devices.⁶ The drawback to this approach is the phase separation of different components, which reduces device lifetimes. From the molecular design aspect, many efforts have been attempted to develop novel materials with improved electron-transporting ability to allow for a fabrication of single-layer devices. In 1989, it was reported that 2-(biphenyl-4-yl)-5-(4-*tert*-butylphenyl)-1,3,4-oxadiazole (PBD) possesses good electron-transporting and emissive properties.⁷ Since this report, oxadiazole (OXD) moieties have been demonstrated to show a high potential as an electron-transporting unit in the study of polymer LEDs.⁸ One useful approach for fabrication of simple and efficient single-layer devices is to employ polymers containing an OXD unit and a hole-transporting unit.⁹

In recent years, LEDs based on conjugated polymers exhibiting polarized emission have attracted much attention because of their potential as backlights for conventional liquid crystal (LC) displays.¹⁰ The introduction of molecular alignment into emissive layers is one of the most promising approaches for elaborate control of emission properties in thin films. The approach to such a device is based on the use of organic materials that are optically anisotropic and can be aligned into a specific direction. LC materials have been widely used as active media in display devices and spatial light modulators. LCs are typical self-organizing materials with unique properties. For example, the self-organized structures are controlled by the choice of phases of LC materials, so that structurally controlled thin films could be prepared by quenching from appropriate fluid phases into solid states. Due to these properties, LC materials are expected to be used not only in display devices but also in various photonic applications.¹¹ Furthermore, LCs possess high carrier-transporting ability.¹² In relation to the carrier transport in polymer liquid crystals (PLCs), a high carrier mobility over 10^{-3} cm²/Vs was reported, which was independent of the electric fields.^{12d} In addition, LEDs based on PLCs showing carrier-transporting properties were reported, which directly emit polarized light: poly(arylenevinylene)¹³ and poly(fluorene)¹⁴ derivatives.

Typical thermotropic LCs are usually composed of two major structural parts: an elongated rigid aromatic core and terminal flexible alkyl chains. Low-molecular-weight and polymer LCs have been reported, in which OXD moieties act as a mesogenic core.¹⁵ To achieve LED performance for a single-layer device, a chromophore with the OXD moiety and a hole-transporting unit would be appropriate. We consider that if an emissive moiety possesses both electron- and hole-transporting segments, it could exhibit ambipolar carrier-transporting ability. We recently reported that a novel π -conjugated compound (**7-OXD-Me**), which contains the OXD moiety as an electron-transporting unit and an amine moiety as a hole-transporting unit, exhibits LC behavior and strong blue fluorescence.¹⁶ **7-OXD-Me** shows a nematic (N) phase between 138 °C and 143 °C. LEDs usually comprise thin-film structures with a thickness less than 100 nm, sandwiched between two electrodes. However, LEDs consisting of low-molecular-weight LCs always require a glass cell,¹⁷ so that these LCs are not necessarily promising from the standpoint

of preparation of thin films. On the basis of these results, we assumed that PLCs with OXD moieties possess a high ability of structurally controlled thin films. We explored electrochemical and EL properties of PLC, **PM6OXDMA**, which is composed of OXD and amine units in the same side chain. We evaluated polarized EL behavior from self-organizing alignment of the PLC.

Experimental Section

The compounds synthesized were identified by means of ¹H NMR (Bruker, model AM200) and ¹³C NMR (JEOL, model JNM-LA300). Molecular weight was determined by gel permeation chromatography (GPC; JASCO, model DG-980-50; column, Shodex GPC K802 + K804 + K805; eluent, chloroform) calibrated with standard polystyrenes. Absorption spectra were measured using a JASCO model U-550. Photoluminescence (PL) and EL spectra were obtained using a Hitachi F-4010 luminescence spectrometer. Fluorescence quantum yield of the polymer was determined by using quinine sulfate as a standard compound.¹⁸

For the steady-state photocurrent measurements, a Xe lamp (500 W) equipped with a band-pass filter (Toshiba, model UV33DS) was used for UV irradiation from 380 to 300 nm. Light intensity was 2.5 mW/cm². The photocurrent was recorded with a source measurement unit (Advantest, model R8340). For transit photocurrent measurements, a conventional time-of-flight (TOF) setup was used with a N₂ laser (337 nm, 40 μ J/pulse, pulse width: 600 ps). The signals were amplified and recorded with a digital oscilloscope (Nicolet, model Pro92). The sample studied here was prepared by casting the polymer solution in 1,2-dichloroethane (2 wt %) onto indium–tin-oxide (ITO) coated glass substrates. The film thickness was 3.3 μ m, measured with a Dektak surface profiler. The film was annealed at 150 °C for 1 h and then cooled to a glassy state. Finally, a semitransparent aluminum electrode of 20 nm thickness was deposited by thermal evaporation at 2×10^{-6} Torr through a shadow mask onto the film yielding sandwich structures with an active area, defined by the electrode overlap, of 40 mm².

Cyclic voltammetry (CV) was performed on an ALS/chi model 600A electrochemical analyzer in a solution of tetraethylammonium tetrafluoroborate (0.1 M) in acetonitrile at a scan rate of 100 mV/s. The polymer film as a working electrode was coated on a square platinum electrode (1 cm²) by casting and then dried in air. CV in a solution was carried out using a platinum disk (1.6 mm in diameter) as the working electrode. Platinum wire was used as a counter electrode, and Ag/AgNO₃ (0.01 M in acetonitrile) electrode was used as a reference electrode. Prior to each series of measurements, the cell was deoxygenated with argon.

To fabricate single-layer LEDs, a polymer layer (thickness: \sim 100 nm) was obtained by spin-coating at a rate of 2500 rpm for 30 s with 1 wt % solution in chloroform. Sample thickness was checked by a Dektak surface profiler. Top contact of MgAg (thickness: 300 nm) was deposited by vacuum evaporation at a pressure of less than 10^{-5} Torr. The emitting area was approximately 4 mm².

Characterization of LCs. LC and phase-transition behavior was examined on an Olympus Model BH-2 polarizing microscope equipped with Mettler hot-stage models FP-90 and FP-82. Thermotropic properties of LCs were determined with a differential scanning calorimeter (Seiko I&E, models SSC-5200 and DSC220C) at a heating rate of 10 °C/min. The LC phase was determined by X-ray diffractometry (MAC Science MXP 3, model 5301; Cu K α 1 radiation from a 1.6 kW anode X-ray

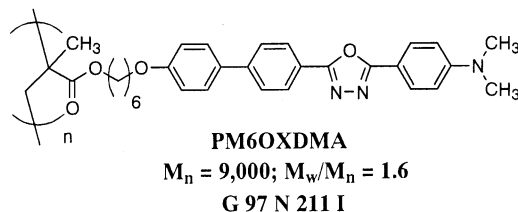


Figure 1. Chemical structure and properties of **PM6OXDMA** used in this study. G, glass; N, nematic; I, isotropic; M_n , number-average molecular weight; and M_w , weight-average molecular weight.

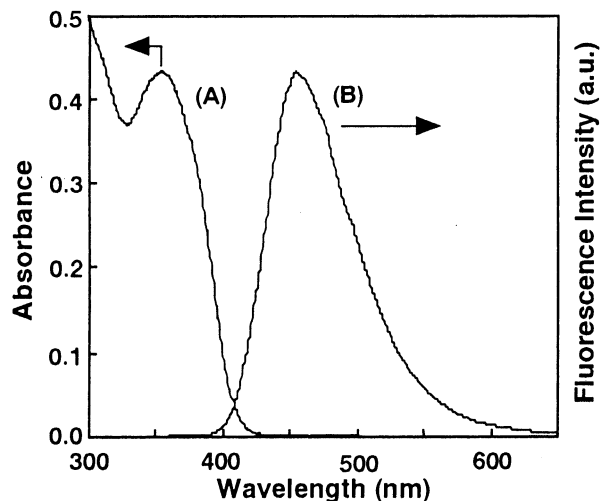


Figure 2. Absorption and photoluminescence spectra of **PM6OXDMA** in a film. (A) Absorption and (B) photoluminescence. Excitation wavelength: 353 nm.

generator at 160 °C). In addition, to determine decomposition temperature of the polymer, thermogravimetry (TG) was conducted with a Seiko I&E model TG/DTA-6200 thermal analysis station.

Results and Discussion

The synthetic details for the OXD monomer and the polymer will be reported elsewhere.¹⁹ The number-average molecular weight M_n of **PM6OXDMA** determined by GPC was 9000 with a polydispersity index of 1.6 as shown in Figure 1.

We observed two endothermic events in DSC on heating: one is due to glass transition temperature T_g at 97 °C and the other corresponds to an N to isotropic (I) phase transition (T_{NI}) at 211 °C (Figure 1). It is worth mentioning here that a significant difference in the LC behavior between the polymer and the low-molecular-weight LC was observed for the same rigid core with an alkyl tail. As described above, **PM6OXDMA** showed the T_{NI} at 211 °C and the temperature range of the N phase with 114 °C on heating, while **7-OXD-Me** exhibited the T_{NI} at 143 °C and a narrow LC temperature range (5 °C on cooling).¹⁶ The origin of the superior LC behavior of the PLC is not fully understood at the present stage of research; however, it is at least true that the polymer plays an important role in the thermal stability of the LC phases and the formation of structurally controlled thin films. Furthermore, it was found that decomposition temperature (395 °C) of **7-OXD-Me** was the same as that of **PM6OXDMA**. These results indicate that the polymer does not decompose on heating under the present DSC analytical conditions.

Optical Properties. Figure 2 shows absorption and PL spectra of **PM6OXDMA** in a film.

The film was prepared by spin-coating from a chloroform solution onto a glass substrate. Maximum absorption wave-

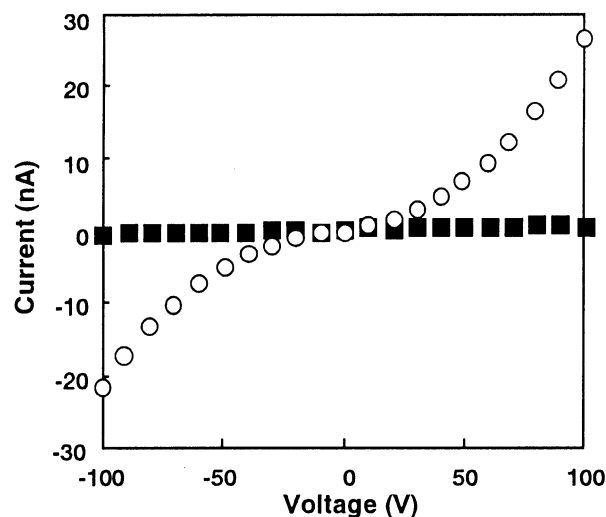


Figure 3. Current-voltage characteristics of photo (circle) and dark (square) currents of **PM6OXDMA** at room temperature. Sample thickness: 3.3 μm .

length λ_{max} of **PM6OXDMA** was 353 nm, which is attributed to the π -conjugated OXD segment. The energy band gap of **PM6OXDMA** calculated from the absorption edge is 2.88 eV. **PM6OXDMA** showed blue fluorescence with an emission peak at 458 nm (excitation wavelength: 353 nm). The PL quantum yield of **PM6OXDMA** in dichloromethane was found to be 0.60. This value is higher than that of typical polymer materials for LED, poly[2-methoxy-5-(2-ethylhexoxy)-1,4-phenylenevinylene] (MEH-PPV, ~ 0.18) and poly(*p*-phenylenevinylene) (PPV, ~ 0.27).^{1b} From the consideration of the PL quantum yield, **PM6OXDMA** may be promising for the application as polymer LEDs.

Carrier-Transporting Property. Steady-state and transit photocurrent measurements were carried out to study the carrier transport properties in a film of **PM6OXDMA**. The steady-state photocurrent involves photogeneration of charge carriers and their transport, which is governed by carrier lifetime and mobility in the film and often by the contact with electrode materials.²⁰ To establish a single-carrier condition in the transport, we selected the irradiation light wavelength shorter than 400 nm, where the penetration depth is estimated to be sufficiently smaller than the film thickness. According to the sign of the applied bias to the illuminated electrode, aluminum in this case, either photogenerated electrons or holes drift under an external bias to the collecting electrode and result in the photocurrent that is monitored with a source measurement unit. Thus, among the factors that determined LED materials capability, the steady-state photocurrents provide us with clear information about the carrier-transport ability of **PM6OXDMA**. Figure 3 shows current-voltage characteristics of photo and dark currents in a film at room temperature.

The dark conductivity of **PM6OXDMA** was estimated to be 3.8×10^{-14} S/cm. Despite asymmetric electrodes, there was little difference in the photocurrent as a function of the applied bias irrespective of its sign. This result indicates that both electrons and holes can be transported in the **PM6OXDMA** film. Furthermore, we estimated the carrier mobility of the polymer using time-of-flight (TOF) method. The carrier mobility could not be determined from transit photocurrent curves at room temperature because of highly dispersive transport, but we observed nondispersive hole transport at 130 °C, whose mobility was determined to be $\mu_p = 2.0 \times 10^{-6}$ cm²/Vs at a field of 9.1×10^5 V/cm. However, electron transient photo-

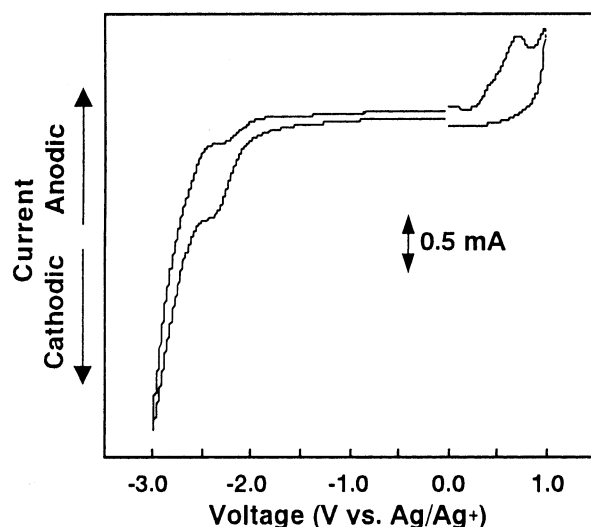


Figure 4. Cyclic voltammogram of PM6OXDMA coated on a platinum electrode in acetonitrile.

currents were still so dispersive at that temperature that we could not determine the electron mobility. This indicates a rather broad distribution of the density of states in PM6OXDMA, especially for electrons. A further detailed investigation of the carrier transport in PM6OXDMA using the TOF technique is now in progress, which includes its temperature and electric field dependences and will be reported later.

Electrochemical Properties. CV was used to estimate relative ionization potentials I_p 's and electron affinities E_A 's of the conjugated chromophore in the side chain. To a first approximation, the oxidation potential of a material (as measured by CV) can be related to the I_p and the highest occupied molecular orbital (HOMO) energy level. A similar relationship may be made with the reduction potential, as well as with the E_A and the lowest unoccupied molecular orbital (LUMO) energies. However, the presence of solvent and counterions, as well as the kinetic nature of electrode processes in CV, make the correlation only approximate. One check on the reliability of this relationship is that the difference between the oxidation potential and the reduction potential should be equal to the optical band gap. Cyclic voltammograms of PM6OXDMA are shown in Figure 4.

PM6OXDMA exhibited the cathodic and the corresponding anodic wave at -2.40 V and -2.33 V vs Ag/Ag⁺. The reduction of the polymer film was accompanied by the change in color from pale yellow to dark red. In contrast to the observation of a redox cycle in the reduction process, scanning to the oxidation process was irreversible. The band gap of PM6OXDMA was estimated to be 3.1 eV from the cyclic voltammograms; it was slightly larger than that obtained from the absorption edge. These results agree with the observation that redox reactions on thin films generally occur at higher oxidation and reduction potentials.²¹

HOMO and LUMO energy levels were determined from the potentials in the CV. We selected PBD and *N,N*-dimethylaniline (DMA) as model compounds and compared the redox property of PM6OXDMA with the model system. The cyclic voltammogram of the model system with PBD/DMA = 1:1 (mol/mol) was measured on a platinum electrode in acetonitrile against the Ag/Ag⁺ reference electrode. The results were compared with the ferrocene/ferrocenium (FOC) couple measured in the same solution. The half-wave oxidation potential $E_{1/2}$ of the FOC was 0.08 V vs Ag/Ag⁺. LUMO levels versus the vacuum level were derived from the measured potentials by assuming that the

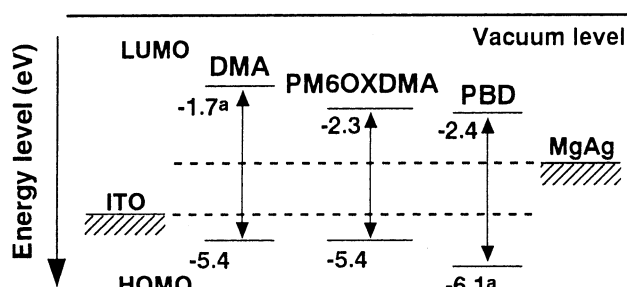


Figure 5. Relative energy levels of DMA, PM6OXDMA, and PBD. HOMO and LUMO levels were converted from measured electrochemical potentials assuming the absolute energy level of ferrocene (FOC) to be -4.8 eV. ^aDetermined from the absorption edge.

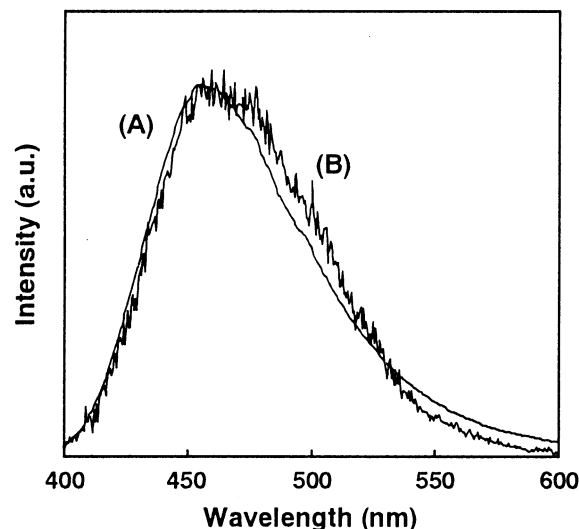


Figure 6. Photoluminescence and electroluminescence spectra of PM6OXDMA. (A) Photoluminescence and (B) electroluminescence. Measured from the device with the configuration of ITO/PM6OXDMA/MgAg.

energy level of FOC is -4.8 eV below the vacuum level.^{6e,22} The HOMO–LUMO energy levels of PM6OXDMA, DMA, and PBD versus vacuum level are shown in Figure 5.

PM6OXDMA and the model system showed similar redox behavior. It is clear that the polymer possessing the OXD moiety and the amine moiety has no inhibitory effect on the carrier-transporting abilities.

Light-Emitting Diodes with the Polymer. It was found that PM6OXDMA is a good candidate for single-layer LED devices because it combines electron-transporting, hole-transporting, and light-emitting properties in a single species. We fabricated polymer LEDs with a simple configuration of ITO/PM6OXDMA/MgAg to demonstrate EL behavior. PL and EL spectra of PM6OXDMA are shown in Figure 6.

The diode emitted visible light above threshold voltages. The EL spectra resembled its PL spectra, suggesting that the same excited state is responsible for both emissions. Figure 7 shows current–voltage and luminance–voltage curves for the single-layer LED at room temperature.

The emission started at a driving voltage of 10 V. Similar turn-on voltages for both the current density and the luminance were observed, indicating balanced charge injection from the cathode and the anode. The device exhibited a maximum luminance of 13 cd/m² at 26 V with an LED quantum efficiency of 3×10^{-4} %²³ (20 V). Some groups reported side-chain polymers with PBD used for the fabrication of LEDs.^{8c,23}

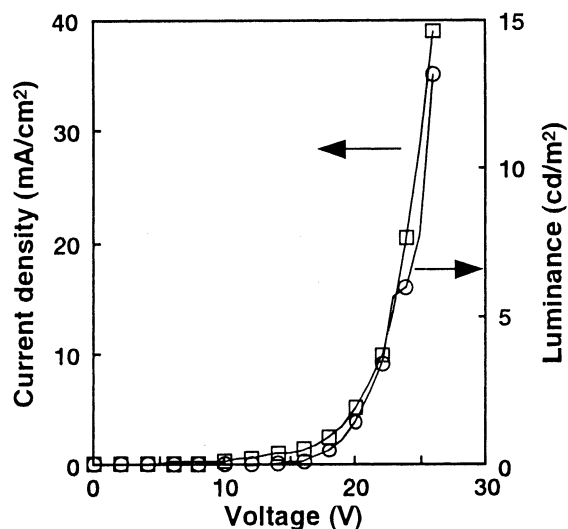


Figure 7. Current–voltage (square) and luminance–voltage (circle) characteristics of the single-layer LED of **PM6OXDMA**. Measurements were performed at room temperature.

Unfortunately, light emission could not be detected from single-layer LEDs of the polymers except multilayer LEDs with PPV as a hole-transporting material. Furthermore, the resulting multilayer LEDs showed a very high value (28 V) of the turn-on voltage.^{8c}

To check the charge-transporting properties of **PM6OXDMA**, we fabricated single-layer LEDs using only electron-transporting moiety or both hole- and electron-transporting moieties. We selected PBD and DMA as model compounds and poly(methyl methacrylate) (PMMA) as a matrix polymer. In the PBD/PMMA mixture, no phase separation was observed up to the PBD fraction of 30 wt %. We fabricated a single-layer LED, ITO/PBD/PMMA (100 nm)/MgAg system. However, EL emission was not observed over 30 V. Moreover, we investigated EL behavior of the PBD/DMA = 1:1 (mol/mol) mixture. Transparent films were obtained at the PBD/DMA concentration up to 30 wt %. An ITO/PBD/DMA/PMMA (100 nm)/MgAg device showed a turn-on voltage at 17 V and reached a brightness of 2 cd/m² at 32 V. We believe that the introduction of the amine into the OXD moiety has two effects. One is to provide a site for hole injection, because OXD moieties are rather electron acceptors. The other effect of amine is to lower the energy level of the polymer HOMO, thus facilitating hole-injection and -transport processes. These results indicate that **PM6OXDMA** with amine and OXD moieties in the same side chain possesses not only carrier-transporting abilities but also an EL character from a single-layer LED as a simple device configuration. We performed device fabrications and characterizations in air without taking any precautions. Higher quantum efficiency could be achieved with optimization of the fabrication conditions.

To make use of distinct properties of **PM6OXDMA** and to investigate potential utility for applications in LEDs, we prepared aligned thin films of the PLC by using a rubbing technique. A preferential alignment was induced in the PLC coated onto a directly rubbed glass substrate with cloth. The film was annealed for 1 h at 150 °C in an N phase, and then cooled to a glassy state. To estimate the degree of alignment achieved in the side chain, polarized absorption and PL were measured. The absorption was recorded with a polarizer placed parallel and perpendicular to the rubbing direction (Figure 8).

The chromophore was aligned predominantly along the rubbing direction. The order parameter $S = \frac{1}{2}\langle 3 \cos^2 \theta \rangle$, where θ denotes the angle between the locally preferred direction and

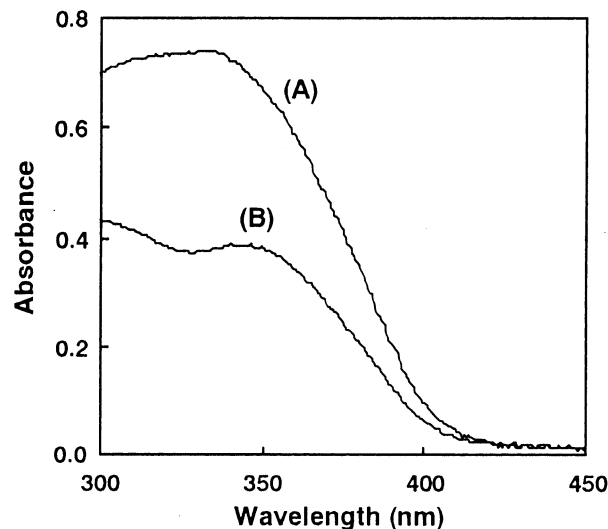


Figure 8. Polarized absorption spectra of **PM6OXDMA** aligned on a rubbed glass substrate. (A) Parallel and (B) perpendicular to the rubbing direction.

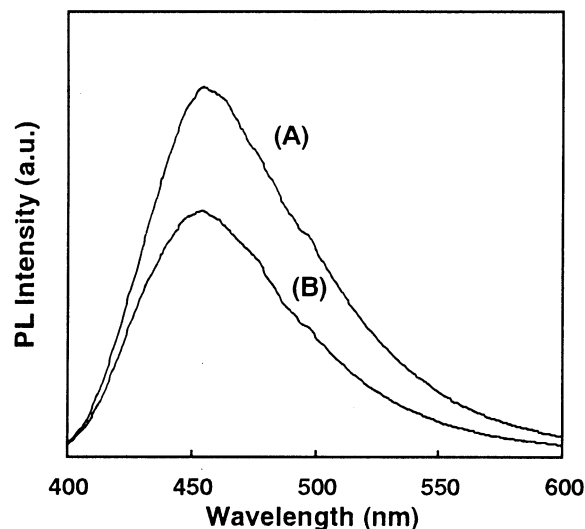


Figure 9. Polarized photoluminescence spectra of **PM6OXDMA** aligned on a rubbed glass substrate. (A) Parallel and (B) perpendicular to the rubbing direction. Excitation wavelength: 345 nm.

the molecular long axis, can be determined from experimental data by the following equation:

$$S = \frac{R - 1}{R + 2}$$

where $R = A_{\parallel}/A_{\perp}$ is a dichroic ratio with A_{\parallel} and A_{\perp} being the values of the polarized absorption parallel and perpendicular to the rubbing direction. A macroscopic order parameter of $S = 0.21$ was obtained from the dichroic ratio at λ_{\max} (345 nm, $R = 1.8$). Transition dipole moment of the chromophore is, thus, aligned predominantly along the rubbing direction. The absorption spectra in the LC state resembled those obtained from the solution closely; no spectral shift was observed. Dichroic PL behavior of the polymer also confirmed the alignment of the chromophores. Figure 9 shows the polarized PL spectra of **PM6OXDMA**.

The emission intensity of the aligned film turned out to be high along the rubbing direction and low in the direction perpendicular to it, yielding a dichroic ratio $D_{\text{PL}} = I_{\parallel}/I_{\perp}$, where I_{\parallel} and I_{\perp} are values of the intensity of PL parallel and

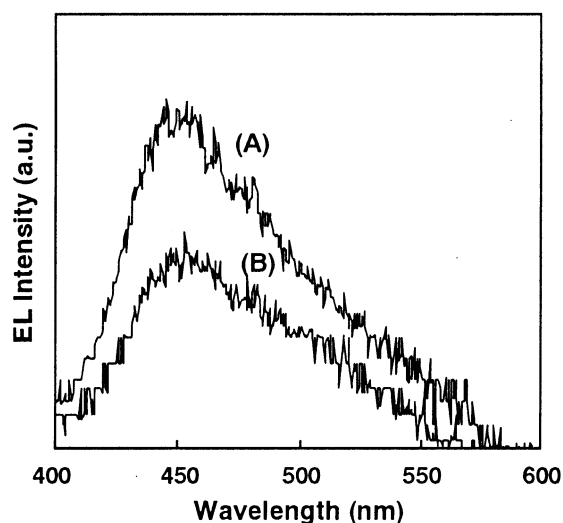


Figure 10. Polarized electroluminescence spectra of **PM6OXDMA** aligned on a rubbed glass substrate with an ITO electrode. (A) Parallel and (B) perpendicular to the rubbing direction. Measured from the device with the configuration of ITO (directly rubbed)/**PM6OXDMA**/MgAg.

perpendicular to the rubbing direction, respectively. D_{PL} was estimated as 1.8 at 458 nm. The single-layer LED consisting of ITO (directly rubbed)/**PM6OXDMA**/MgAg showed polarized EL (Figure 10).

The dichroic ratio calculated from the polarized EL spectra was $D_{EL} = 1.6$. The emission maximum was located at around 460 nm. These results indicate that the transition dipole moments are aligned along the rubbing direction as expected from the results on the PL dichroism. In general, the macroscopic orientation of PLCs at surfaces can be described in the same way as that of low-molecular-weight LCs. However, the alignment behavior of these materials has an influence on the surface property. When the glass substrate is rubbed in one direction, the LC molecules orient preferentially in this direction. It may result from a change in the anchoring direction with respect to the surface region.²⁵ To produce aligned devices, some groups used polyimide as an alignment layer on the top of ITO.^{13,14} In this work, we did not try to optimize the device parameters, such as the alignment layer, carrier injection, and lifetime. However, the polarized EL in simple devices using self-organizing ability of PLCs containing carrier-transporting and emission properties has been clearly demonstrated.

Conclusions

The side-chain PLC containing an OXD moiety as an electron-transporting unit and an amine moiety as a hole-transporting unit showed stable LC behavior in comparison with the low-molecular-weight OXD analogues. We found that the polymer combines carrier-transporting and emission properties in a single species. Furthermore, it was clear that the polymer possessing OXD and amine moieties in the same side chain shows no inhibitory effect on the carrier-transporting abilities. We fabricated polymer LEDs with a simple configuration of ITO/PLC/MgAg, which showed not only EL emission but also polarized EL by rubbing treatment. These results indicate that the origin of the polarized emission in the polymer films is the anisotropic arrangement of the mesogenic units. Since there are many other efficient hole-transporting moieties, which can be connected with the OXD unit, we expect new PLCs with good LED performance to be further developed in this line of molecular design.

Acknowledgment. The authors thank Professor Jun-ichi Hanna and Mr. Hiroaki Iino at Tokyo Institute of Technology for steady-state and transit photocurrent measurements and useful suggestions.

References and Notes

- (1) For reviews, see: (a) Kraft, A.; Grimsdale, A. C.; Holmes, A. B. *Angew. Chem., Int. Ed.* **1998**, *37*, 402–428. (b) Friend, R. H.; Gymer, R. W.; Holmes, A. B.; Burroughes, J. H.; Marks, R. N.; Taliani, C.; Bradley, D. D. C.; Dos Santos, D. A.; Brédas, J. L.; Lögdlund, M.; Salaneck, W. R. *Nature* **1999**, *397*, 121–128. (c) Shirota, Y. *J. Mater. Chem.* **2000**, *10*, 1–25. (d) Kim, D. Y.; Cho, H. N.; Kim, C. Y. *Prog. Polym. Sci.* **2000**, *25*, 1089–1139. (e) Mitschke, U.; Bäuerle, P. *J. Mater. Chem.* **2000**, *10*, 1471–1507.
- (2) Tang, C. W.; VanSlyke, S. A. *Appl. Phys. Lett.* **1987**, *51*, 913–915.
- (3) (a) Shirota, Y.; Kuwabara, Y.; Ianada, H.; Wakimoto, T.; Nakada, H.; Yonemoto, Y.; Kawami, S.; Imai, K. *Appl. Phys. Lett.* **1994**, *65*, 807–809. (b) Shirota, Y.; Kuwabara, Y.; Okuda, D.; Okuda, R.; Ogawa, H.; Inada, H.; Wakimoto, T.; Nakada, H.; Yonemoto, Y.; Kawami, S.; Imai, K. *J. Lumin.* **1997**, *72–75*, 985–991. (c) Noda, T.; Shirota, Y. *J. Am. Chem. Soc.* **1998**, *120*, 9714–9715. (d) Noda, T.; Ogawa, H.; Shirota, Y. *Adv. Mater.* **1999**, *11*, 283–285. (e) Shirota, Y.; Kinoshita, M.; Noda, T.; Okumoto, K.; Ohara, T. *J. Am. Chem. Soc.* **2000**, *122*, 11021–11022. (f) Okumoto, K.; Ohara, T.; Noda, T.; Shirota, Y. *Synth. Met.* **2001**, *121*, 1655–1656.
- (4) (a) Burroughes, J. H.; Bradley, D. D. C.; Brown, A. R.; Marks, R. N.; Mackay, K.; Friend, R. H.; Burns, P. L.; Holmes, A. B. *Nature* **1990**, *347*, 539–541. (b) Gustafsson, G.; Cao, Y.; Treacy, G. M.; Klavetter, F.; Colaneri, N.; Heeger, A. J. *Nature* **1992**, *357*, 477–479.
- (5) (a) Brown, A. R.; Bradley, D. D. C.; Burn, P. L. J.; Burroughes, H.; Friend, R. H.; Greenham, N.; Kraft, A. *Appl. Phys. Lett.* **1992**, *61*, 2793–2795. (b) Greenham, N. C.; Moratti, S. C.; Bradley, D. D. C.; Friend, R. H.; Holmes, A. B. *Nature* **1993**, *365*, 628–630. (c) Parker, I. D.; Pei, Q.; Marrocco, M. *Appl. Phys. Lett.* **1994**, *65*, 1272–1274. (d) Son, S.; Dodabalapur, A.; Lovinger, A. J.; Galvin, M. E. *Science* **1995**, *269*, 376–378.
- (6) (a) Kido, J.; Kohda, M.; Okuyama, K.; Nagai, K. *Appl. Phys. Lett.* **1992**, *61*, 761–763. (b) Zhang, C.; von Seggern, H.; Kraabel, B.; Schmidt, H.-W.; Heeger, A. J. *Synth. Met.* **1995**, *72*, 185–188. (c) Kido, J.; Shionoya, H.; Nagai, K. *Appl. Phys. Lett.* **1995**, *67*, 2281–2283. (d) Birgersson, J.; Kaeriyama, K.; Barta, P.; Bröms, P.; Fahlman, M.; Granlund, T.; Salaneck, W. R. *Adv. Mater.* **1996**, *8*, 982–985. (e) Wu, C. C.; Sturm, J. C.; Register, R. A.; Tian, J.; Dana, E. P.; Thompson, M. E. *IEEE Trans. Electron Devices* **1997**, *44*, 1269–1281.
- (7) Adachi, C.; Tsutsui, T.; Saito, S. *Appl. Phys. Lett.* **1989**, *55*, 1489–1491.
- (8) (a) Pei, Q.; Yang, Y. *Adv. Mater.* **1995**, *7*, 559–561. (b) Buchwald, E.; Meier, M.; Karg, S.; Pösch, P.; Schmidt, H.-W.; Strohrriegel, P.; Riess, W.; Schwoerer, M. *Adv. Mater.* **1995**, *7*, 839–842. (c) Strukelj, M.; Papadimitrakopoulos, F.; Miller, T. M.; Rothberg, L. J. *Science* **1995**, *267*, 1969–1972. (d) Kim, S. T.; Hwang, D.; Li, X. C.; Grüner, J.; Friend, R. H.; Holmes, A. B.; Shim, H. K. *Adv. Mater.* **1996**, *8*, 979–982. (e) Cao, Y.; Parker, I. D.; Yu, G.; Zhang, C.; Heeger, A. J. *Nature* **1999**, *397*, 414–417.
- (9) (a) Huang, W.; Yu, W.-L.; Meng, H.; Pei, J.; Li, S. F. Y. *Chem. Mater.* **1998**, *10*, 3340–3345. (b) Peng, Z.; Bao, Z.; Galvin, M. E. *Adv. Mater.* **1998**, *10*, 680–684. (c) Chung, S.-J.; Kwon, K.-Y.; Lee, S.-W.; Jin, J.-I.; Lee, C. H.; Lee, C. E.; Park, Y. *Adv. Mater.* **1998**, *10*, 1112–1116. (d) Bao, Z.; Peng, Z.; Galvin, M. E.; Chandross, E. A. *Chem. Mater.* **1998**, *10*, 1201–1204. (e) Peng, Z.; Bao, Z.; Galvin, M. E. *Chem. Mater.* **1998**, *10*, 2086–2090. (f) Peng, Z.; Zhang, J. *Chem. Mater.* **1999**, *11*, 1138–1143. (g) Song, S.-Y.; Jang, M.-S.; Shim, H.-K.; Hwang, D.-H.; Zyung, T. *Macromolecules* **1999**, *32*, 1482–1489. (h) Pei, J.; Yu, W.-L.; Huang, W.; Heeger, A. J. *Macromolecules* **2000**, *33*, 2462–2471. (i) Song, S.-Y.; Ahn, T.; Shim, H.-K.; Song, I.-S.; Kim, W.-H. *Polymer* **2001**, *42*, 4803–4811. (j) Pei, J.; Yu, W.-L.; Ni, J.; Lai, Y.-H.; Heeger, A. J. *Macromolecules* **2001**, *34*, 7241–7248. (k) Lee, Y.-Z.; Chen, X.; Chen, S.-A.; Wei, P.-K.; Fann, W.-S. *J. Am. Chem. Soc.* **2001**, *123*, 2296–2307.
- (10) (a) Lüssem, G.; Wendorff, J. H. *Polym. Adv. Technol.* **1998**, *9*, 443–460. (b) Grell, M.; Bradley, D. C. *Adv. Mater.* **1999**, *11*, 895–905.
- (11) (a) Ikeda, T.; Tsutsumi, O. *Science* **1995**, *268*, 1873–1875. (b) Shishido, A.; Tsutsumi, O.; Kanazawa, A.; Shiono, T.; Ikeda, T.; Tamai, N. *J. Am. Chem. Soc.* **1997**, *119*, 7791–7796. (c) Lee, H. K.; Kanazawa, A.; Shiono, T.; Ikeda, T.; Fujisawa, T.; Aizawa, M.; Lee, B. *Chem. Mater.* **1998**, *10*, 1402–1407. (d) Wu, Y.; Demachi, Y.; Tsutsumi, O.; Kanazawa, A.; Shiono, T.; Ikeda, T. *Macromolecules* **1998**, *31*, 349–354. (e) Ogiri, S.; Kanazawa, A.; Shiono, T.; Ikeda, T.; Nishiyama, I.; Goodby, J. W. *Macromolecules* **1998**, *31*, 1728–1734. (f) Hasegawa, M.; Yamamoto, T.; Kanazawa, A.; Shiono, T.; Ikeda, T. *Adv. Mater.* **1999**, *11*, 675–677. (g)

- Yamamoto, T.; Hasegawa, M.; Kanazawa, A.; Shiono, T.; Ikeda, T. *J. Phys. Chem. B* **1999**, *103*, 9873–9878. (h) Zhang, H.; Shiino, S.; Shishido, A.; Kanazawa, A.; Tsutsumi, O.; Shiono, T.; Ikeda, T. *Adv. Mater.* **2000**, *12*, 1336–1338. (i) Yoneyama, S.; Yamamoto, T.; Hasegawa, M.; Kanazawa, A.; Shiono, T.; Ikeda, T. *J. Mater. Chem.* **2001**, *11*, 3008–3013.
- (12) (a) Adam, D.; Schuhmacher, P.; Simmerer, J.; Häussling, L.; Siemensmeyer, K.; Eitzbach, K.; Ringsdorf, H.; Haarer, D. *Nature* **1994**, *371*, 141–143. (b) Funahashi, M.; Hanna, J. *Phys. Rev. Lett.* **1997**, *78*, 2184–2187. (c) Tokuhisa, H.; Era, M.; Tsutsui, T. *Adv. Mater.* **1998**, *10*, 404–407. (d) Redecker, M.; Bradley, D. D. C.; Inbasekaran, M.; Woo, E. P. *Appl. Phys. Lett.* **1998**, *73*, 1565–1567.
- (13) (a) Lüssem, G.; Geffarth, F.; Greiner, A.; Heitz, W.; Hopmeier, M.; Oberski, M.; Unterlechner, C.; Wendorff, J. H. *Liq. Cryst.* **1996**, *21*, 903–907. (b) Oberski, J. M.; Clauswitz, K. U.; Lüssem, G.; Geffarth, F.; Wendorff, J. H.; Greiner, A. *Macromol. Symp.* **2000**, *154*, 235–244. (c) Clauswitz, K.-U. W.; Geffarth, F.; Greiner, A.; Lüssem, G.; Wendorff, J. H. *Synth. Met.* **2000**, *111–112*, 169–171.
- (14) (a) Grell, M.; Knoll, W.; Lupo, D.; Meisel, A.; Miteva, T.; Neher, D.; Nothofer, H. G.; Scherf, U.; Yasuda, A. *Adv. Mater.* **1999**, *11*, 671–675. (b) Grell, M.; Redecker, M.; Whitehead, K. S.; Bradley, D. D. C.; Inbasekaran, M.; Woo, E. P.; Wu, W. *Liq. Cryst.* **1999**, *26*, 1403–1407. (c) Whitehead, K. S.; Grell, M.; Bradley, D. D. C.; Inbasekaran, M.; Woo, E. P. *Synth. Met.* **2000**, *111–112*, 181–185. (d) Miteva, T.; Meisel, A.; Grell, M.; Nothofer, H. G.; Lupo, D.; Yasuda, A.; Knoll, W.; Kloppenburg, L.; Bunz, U. H. F.; Scherf, U.; Neher, D. *Synth. Met.* **2000**, *111–112*, 173–176. (e) Neher, D. *Macromol. Rapid Commun.* **2001**, *22*, 1366–1385.
- (15) (a) Girdziunaite, D.; Tschierske, C.; Novotna, E.; Kresse, H.; Hetzheim, A. *Liq. Cryst.* **1991**, *10*, 397–407. (b) Tokuhisa, H.; Era, M.; Tsutsui, T. *Chem. Lett.* **1997**, 303–304. (c) Thünemann, A. F.; Janietz, S.; Anlauf, S.; Wedel, A. *J. Mater. Chem.* **2000**, *10*, 2652–2656.
- (16) Mochizuki, H.; Hasui, T.; Kawamoto, M.; Shiono, T.; Ikeda, T.; Adachi, C.; Taniguchi, Y.; Shirota, Y. *Chem. Commun.* **2000**, 1923–1924.
- (17) (a) Tokuhisa, H.; Era, M.; Tsutsui, T. *Appl. Phys. Lett.* **1998**, *72*, 2639–2641. (b) Kogo, K.; Goda, T.; Funahashi, M.; Hanna, J. *Appl. Phys. Lett.* **1998**, *73*, 1595–1597.
- (18) Demas, J. N.; Crosby, G. A. *J. Phys. Chem.* **1971**, *75*, 991–1024.
- (19) Mochizuki, H.; Hasui, T.; Kawamoto, M.; Shiono, T.; Ikeda, T.; Adachi, C.; Taniguchi, Y.; Shirota, Y. In preparation.
- (20) (a) Funahashi, M.; Hanna, J. *Jpn. J. Appl. Phys.* **1996**, *35*, L703–L705. (b) Funahashi, M.; Hanna, J. *Jpn. J. Appl. Phys.* **1999**, *38*, L132–L135.
- (21) (a) Meerholz, K.; Gregorius, H.; Müllen, K.; Heinze, J. A. M. *Adv. Mater.* **1994**, *6*, 671–674. (b) Janietz, S.; Bradley, D. D. C.; Grell, M.; Giebeler, C.; Inbasekaran, M.; Woo, E. P. *Appl. Phys. Lett.* **1998**, *73*, 2453–2455. (c) Chen, Z.-K.; Meng, H.; Lai, Y.-H.; Huang, W. *Macromolecules* **1999**, *32*, 4351–4358.
- (22) (a) Pommerehne, J.; Vestweber, H.; Guss, W.; Mahrt, R. F.; Bäessler, H.; Porsch, M.; Daub, J. *Adv. Mater.* **1995**, *7*, 551–554. (b) Janietz, S.; Wedel, A. *Adv. Mater.* **1997**, *9*, 403–407.
- (23) External quantum efficiency η_φ was determined according to the following equation:
- $$\eta_\varphi = \frac{\pi L \int \frac{F'(\lambda) \lambda}{hc} d\lambda}{K_m \int F'(\lambda) y(\lambda) d\lambda} \frac{e}{J}$$
- where L is the measured forward directed luminance (cd/m^2), J is the measured current density (A/m^2), K_m is the maximum luminous efficiency (namely, 680 lm/W), $y(\lambda)$ is the normalized photonic spectral response function, $F'(\lambda)$ is the EL emission spectrum for the device, and λ is wavelength.
- (24) Cacialli, F.; Li, X.-C.; Friend, R. H.; Moratti, S. C.; Holmes, A. B. *Synth. Met.* **1995**, *75*, 161–168.
- (25) D. Demus, D.; Goodby, J.; Gray, G. W.; Spiess, H.-W. *Handbook of Liquid Crystals*; Wiley: New York, 1998; Vol. 1.